Heliyon 10 (2024) e27767

Contents lists available at ScienceDirect

Heliyon

journal homepage: www.cell.com/heliyon

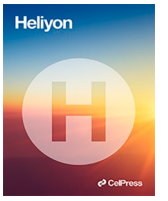

Research article

Corncob-supported calcium oxide nanoparticles from hen eggshells for cadmium (Cd-II) removal from aqueous solutions; Synthesis and characterization

Werkne Sorsa Muleta [a], Sultan Mulisa Denboba [b], Abreham Bekele Bayu [a,c,*]

[a] School of Chemical Engineering, Jimma Institute of Technology, Jimma University, 378, Jimma, Ethiopia
[b] Faculty of Materials Science and Engineering, Jimma Institute of Technology, Jimma University, 378, Jimma, Ethiopia
[c] Faculty of Civil and Environmental Engineering, Gdansk University of Technology, Narutowicza 11/12, 80-233, Gdansk, Poland

ARTICLE INFO

Keywords:
Adsorption
Cadmium
Calcium oxide nanoparticles
Corncob
Hen eggshell
Sol-gel method

ABSTRACT

This study investigated the efficient removal of cadmium ions from aqueous solutions using calcium oxide nanoparticles (CaO NPs) synthesized from waste hen eggshells using a Sol-gel method and supported on corncob bio-adsorbent. The synthesized CaO NPs were characterized using FT-IR, XRD, specific surface area, and TGA. Batch adsorption experiments were conducted to examine the influence of process parameters such as adsorbent dosages, initial Cd (II) concentrations, pH values, and contact times. XRD analysis revealed that the synthesized CaO nanoparticles had a size of 24.34 nm and a specific surface area of 77.4 m^2/g. The optimal conditions for achieving the highest percent removal of cadmium (99.108%) were found to be an initial concentration of 55 ppm, pH 7, adsorbent dose of 0.75 g, and contact time of 50 min. The experimental removal efficiency closely matched the predicted value (99.0%), indicating the suitability of the method used in optimizing the removal of Cd (II) ions from aqueous solutions. These findings, corroborated by predicted values, underscore the efficacy of our method in optimizing cadmium removal. Based on these findings, it can be concluded that corncob-supported CaO NPs are optimized for their highest efficiency and hold great promise as a cost-effective and environmentally friendly solution for wastewater treatment with a focus on cadmium removal.

1. Introduction

Water pollution, which is caused by heavy metal ions from various familiar sources, has instantly become a critical environmental issue. In progressively developing nations, including Ethiopia, industrial discharges of contaminants have led to a significant deterioration in water quality, emerging as a pressing environmental problem [1]. Environmental legislation mandates key industries to progressively eliminate heavy metals from their toxic-containing effluents before proper disposal into river water. However, many low-income industries struggle to typically invest in pollution remediation apparatus and modern technologies [2]. Furthermore, industries that maintain sufficient capital frequently lack interest in implementing efficient treatment technologies due to inadequate governmental control and inadequate environmental policy enforcement. Heavy metal pollution suffers a lasting impact on the

* Corresponding author. School of Chemical Engineering, Jimma Institute of Technology, Jimma University, 378, Jimma, Ethiopia.
E-mail address: abreham.bayu@pg.edu.pl (A.B. Bayu).

https://doi.org/10.1016/j.heliyon.2024.e27767
Received 14 December 2023; Received in revised form 24 February 2024; Accepted 6 March 2024
Available online 12 March 2024

environment, persisting in soil and aqueous solutions without being decomposed like other organic pollutants. Uniquely, the discharge of wastewater containing Cd (II) has led to contaminating both water bodies and land. Cadmium, known for its acute toxicity and persistence, can accumulate in living organisms causing various health issues including kidney damage, bone disorders, and cancer [3].

Various treatment methods have been adopted to separate heavy metals from wastewater, including physical, chemical, and biological approaches [4–6]. Among these methods, adsorption is the most preferred technique due to its simplicity, flexible design, and ease of operation [7]. Commonly used adsorbents such as activated carbon, activated alumina, and ion exchange resins have good pollutant removal capacities. However, their main shortcomings include high installation and operating costs and difficulty in regeneration, thereby increasing the overall wastewater treatment expenses [8]. Therefore, it is crucial to explore alternative approaches that utilize locally available materials to remove heavy metal ions from aqueous solutions. While different forms of biomass have been explored for the removal of cadmium pollutants from various sources of effluents, limited research has been conducted on the use of eggshell-based materials as bio-adsorbents. Moreover, previous studies that utilized raw hen eggshells as adsorbents for heavy metal removal yielded low removal efficiencies due to their lack of porosity and large surface areas. To overcome these limitations, converting used hen eggshells into high-value products, such as calcium oxide nanoparticles, offers a promising alternative method. The synthesis of nanoparticles has gained significant attention due to their improved performance, particularly in terms of enhanced surface area [9]. Calcium oxide (CaO) nanoparticles have shown promising results in this regard. However, the majority of these studies have utilized conventional precursors or commercially available sources for the synthesis of CaO nanoparticles [9–13]. This highlights an important research gap concerning the use of sustainable resources for CaO nanoparticle synthesis.

In this study, the sol-gel method was employed to synthesize CaO nanoparticles from a hen eggshell. The sol-gel method offers the advantages of being cost-effective, easy to implement, and environmentally friendly [10]. Hen eggshell, a well-known agricultural waste material, is disposed of every day on a massive scale by households, restaurants, the food industry, bakery shops, and poultry farms [9]. In Ethiopia, where advanced wastewater treatment methods for managing industrial effluents are not feasible, utilizing resources such as hen eggshells to synthesize calcium oxide nanoparticles becomes essential [14]. These nanoparticles can be employed as adsorbents in heavy metal removal processes within the industrial sector [15]. By utilizing this approach, contaminated wastewater can be effectively treated before its release into the environment and bodies of water, making a significant contribution to mitigating the issue of heavy metal pollution.

Furthermore, while previous research has explored the application of CaO nanoparticles for the removal of heavy metal ions, limited studies have investigated the synergistic use of bio-adsorbents to enhance the efficiency of these nanoparticles. In addition to CaO nanoparticles, the study aimed to investigate the use of corncob as a bio-adsorbent to enhance the performance of the adsorbents in cadmium removal. Utilizing corncob as a support material for CaO nanoparticles provides a sustainable and cost-effective solution for wastewater treatment applications. Corncob possesses several advantageous characteristics as a bio-adsorbent, including its abundance, low cost, and environmentally friendly nature. Its porous structure provides a substantial surface area for effective adsorption, while the presence of functional groups, such as hydroxyl and carboxyl groups, facilitates the binding of heavy metal ions [16]. The incorporation of corncob as a bio-adsorbent in conjunction with CaO nanoparticles offers a unique approach to improving cadmium ion removal. Therefore, this research study focused on bridging this gap by evaluating the effectiveness of the corncob bio-adsorbent in combination with CaO nanoparticles, thereby contributing to the development of eco-friendly and cost-effective methods for water treatment solutions. The main objective of this study was to examine the capability of corncob-supported calcium oxide nanoparticles synthesized from eggshells as an adsorbent for the efficient removal of cadmium ions from aqueous solutions. The effectiveness of these nanoparticles in capturing and immobilizing cadmium ions was assessed, aiming to address the issue of heavy metal contamination in water and wastewater. Several factors influencing the adsorption process, including pH, contact time, and initial concentration of cadmium ions, were thoroughly investigated. Utilization of locally abundant resources for highly effective wastewater treatment and environmental remediation is highly appreciated.

2. Materials and methods

2.1. Materials and chemicals

A wide range of high-quality chemical reagents was utilized in this study for various purposes. These included Cd (II) for preparing standard metal ion samples, sodium hydroxide (NaOH), and hydrochloric acid (HCl) for pH adjustment and to accelerate the gelation process in the synthesis of CaO nanoparticles, 1, 5 diphyl thiocarbazone (dithizone) as a photometric reagent for generating colored water-insoluble complexes with multiple metal ions, $H_2SO_4^-$ for digesting metal ions in the Cadmium nitrate solution, acetone as a solvent for dissolving aqueous salt suspensions for spectrophotometric measurements, and sodium chloride (NaCl) as an electrolyte for determining the point of zero charges of the adsorbent surfaces. All these chemicals and reagents were of analytical grade and were purchased from Wehib Chemicals Trading P.L.C (Addis Ababa, Ethiopia). Distilled water was used to conduct all experiments, and nitrogen gas was employed as an inert atmosphere to prevent sample oxidation during thermal treatment.

2.2. Methods

2.2.1. Sample collection

In the city of Jimma, there is a significant presence of bakeries that produce a substantial amount of eggshells daily. It has been estimated that the average annual production of chicken eggshells by bakeries in Jimma amounts to approximately 94.53 tons [17].

Considering the significant quantity of eggshells produced by the bakeries in Jimma regularly, their accessibility and ease of collection make them a valuable resource that can be utilized effectively for various purposes. This abundance of eggshells presents an opportunity for sustainable and cost-effective solutions in different industries, contributing to the overall development and utilization of available resources in the region. Additionally, corncob samples were collected from local communities in Jimma. The city's corn processing facilities play a vital role in the local agricultural sector, processing a substantial quantity of corn and generating a significant amount of corncobs as a byproduct. The accessibility and availability of corncobs from these processing facilities make them a valuable resource that can be effectively utilized as a bio-adsorbent.

2.2.2. *Synthesis of calcium oxide nanoparticles*

The synthesis of calcium oxide (CaO) nanoparticles from hen eggshells was conducted using the sol-gel method. This method allowed for the synthesis of calcium oxide nanoparticles at ambient temperature, resulting in reduced energy consumption, low cost, absence of additives, shorter preparation time, and no need for pressure [18]. The synthesis process consisted of the following steps.

i. Collection and Preparation of Hen Eggshells: Hen eggshells were collected from local communities, restaurants, bakeries, and broiler chicken farms in Jimma City, Ethiopia. After collecting the eggs, the shells of the chicken eggs were thoroughly washed with tap water to remove dust, impurities, and organic matter adhering to the surface of the eggshells, and then washed several times with distilled water. The well-washed eggshells are then dried in an oven at 150 °C for 3 h to remove moisture and crushed into fine powders using a mortar and pestle [16].
ii. Extraction of Calcium Carbonate ($CaCO_3$): The crushed eggshell powders were added to a container and reacted with an acid solution, hydrochloric acid (HCl), to extract the calcium carbonate ($CaCO_3$) component from the eggshells.
iii. Filtration and Washing: After the extraction, the resulting suspension was filtered using filter paper to separate the calcium carbonate precipitate from the acid solution. The precipitate was then washed with deionized water several times to remove any remaining acid traces and impurities.
iv. Drying and Calcination: The washed calcium carbonate precipitate was dried in an oven at a temperature of 150 °C until a constant weight was achieved. This step ensured the removal of moisture before calcination. The dried precipitate was then calcined in a high-temperature furnace at a temperature of 900 °C for 3 h. The calcination process converted the calcium carbonate into calcium oxide nanoparticles [19].

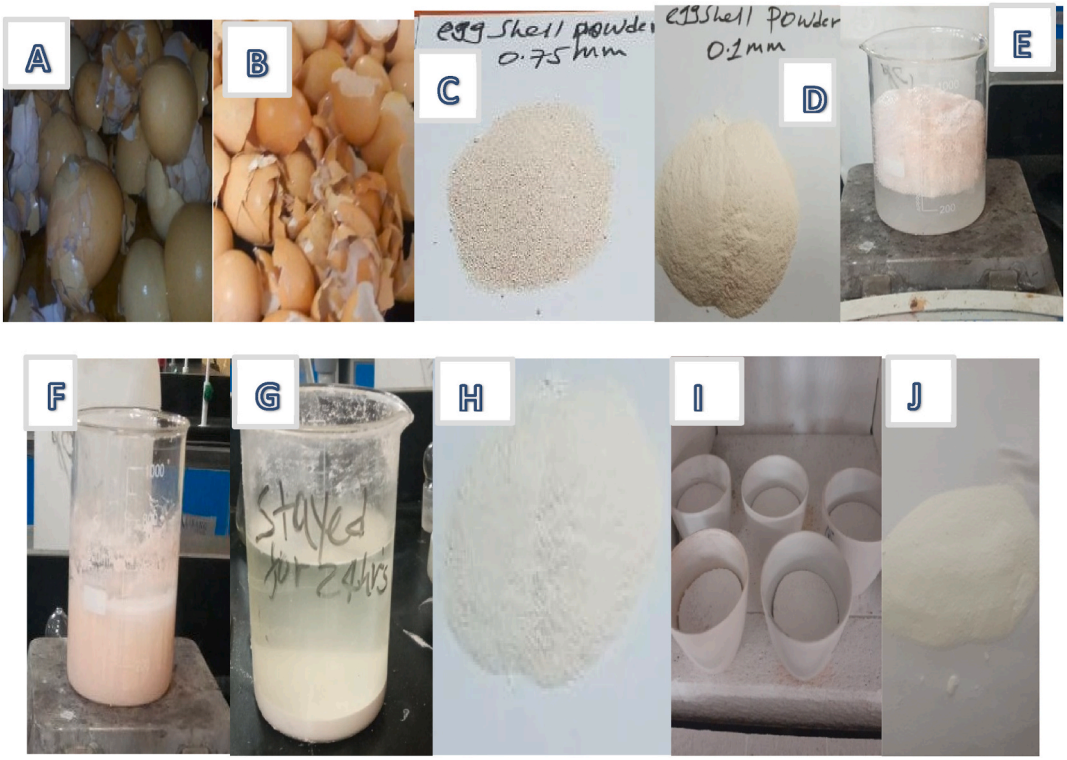

Fig. 1. Synthetization steps of CaO NP adsorbent (Jalu et al. 2021). A) Raw hen eggshells, B) Washed hen eggshells, C) Oven-dried and size-reduced eggshells, D) Sieved eggshells after ground, E) Preparation of homogeneous solutions, F) Hydrolyses reaction, G) Condensation reaction, H) Oven drying of Collection of filtered gels, I) Muffle furnace calcination of dried gels, J) Calcinated Gel powders (CaO NPs)..

v. Grinding and Sieving: The calcined product was ground to a fine powder using a grinding mill. The resulting powder was sieved through a 100 μm mesh to obtain a uniform particle size distribution, typically in the nanoparticle range.

The synthesis steps of CaO nanoparticles are illustrated in Fig. 1 as Fig. 1A) raw hen eggshells, Fig. 1B) washed hen eggshells, Fig. 1C) oven-dried and size-reduced eggshells, Fig. 1D) sieved eggshells after ground, Fig. 1E) preparation of homogeneous solutions, Fig. 1F) hydrolyses reaction, Fig. 1G) condensation reaction, Fig. 1H) oven drying of Collection of filtered gels, Fig. 1I) muffle furnace calcination of dried gels, and Fig. 1J) calcined Gel powders (CaO NPs).The reactions occurring during the synthesis process with constant reaction parameters were carried out using the following procedures:

Making a uniform solution of metallic salt, $CaCl_2$ by dissolving powdered raw eggshell in 36.5% dilute hydrochloric acid. 10.6 g of raw eggshell powder (RESP) was dissolved in 0.25 L of 1 M hydrochloric acid (HCl). This reaction can be represented by Equation (1).

$$ESPCaCo_3(s) + 2HCl\ (aq) \rightarrow CaCl_2(aq) + H_2O\ (l) + CO_{2\ (g)} \quad (1)$$

Sol generation using a hydrolysis reaction. Hydrolysis reactions increase the alkalinity of the system in an aqueous solution [20]. Calcium hydroxide (Ca (OH) $_2$) was produced by the hydrolysis process. 1 M in 250 mL of sodium hydroxide (99% concentration) was added dropwise to convert the solution of calcium chloride produced in Equation (1) above to a sol at room temperature. Gradually adding an aqueous solution of caustic soda to the solution produces precipitates of calcium hydroxide on top of each other, producing a highly crystalline gel. This reaction is represented by Equation (2).

$$CaCl_2\ (aq) + 2Na\ (OH_2)\ (aq) \rightarrow Ca\ (OH)_{2}\ (s) + 2\ NaCl\ (aq) \quad (2)$$

The gel was generated by a condensation reaction. A condensation reaction occurs when two molecules combine to form a larger molecule and release a smaller molecule in the process. Calcium hydroxide, a gel-containing solution stayed for 24 h s at ambient temperature to condense very well. After condensation, the next step involved filtration using a centrifuge at 3000 rpm to obtain a gel of $Ca(OH)_2$.

Finally, the generated precipitate was dried at 150 °C for one day in a heating oven to remove the water. This reaction is shown in Equation (3) below.

$$Ca\ (OH)_2(s) + \Delta \rightarrow CaO(s) + H_2O(l) \quad (3)$$

To enhance the adsorption process, corncob was utilized as a support material alongside the synthesized CaO nanoparticles. The sample preparation and pre-treatment of corncob also involved cleaning, drying, grinding, and sieving. These steps were carried out to ensure the suitability and enhanced properties of corncob as a support material for CaO NPs, enabling the efficient adsorption of cadmium ions using calcium oxide nanoparticles derived from eggshells. The combination of the corncob support material and the synthesized CaO nanoparticles synergistically enhances the overall adsorption capabilities, resulting in an effective and efficient adsorption process.

2.2.3. Calcium oxide nanoparticles supported with corn cob

The preparation of calcium oxide nanoparticles supported with corncob was conducted to develop a mixture of materials, called Corncob Supported Calcium Oxide Nanoparticles (CCS–CaO NPs). The mixture was prepared by incorporating 85% calcium oxide nanoparticles with 15% of the corncob material. This weight ratio was chosen to achieve an optimal distribution of the calcium nanoparticles within the corncob matrix. The composite formulation aimed to capitalize on the combined advantages of both components, ensuring the synergistic effects and improved performance of CCS-CaO NPs in subsequent experimental procedures. After the successful synthesis of CCS-CaO NPs, the mixture was carefully stored in a suitable location to maintain its stability and integrity until further stages of the experiment. This storage ensured that the CCS-CaO NPs retained their desired properties and could be effectively utilized in the adsorption process. This approach enabled the CCS-CaO NPs to benefit from the combined advantages of both components, leading to enhanced performance.

2.2.4. Characterization of eggshell bio-sorbent by proximate analysis

Proximate analysis was used to characterize eggshell bio-sorbent, providing valuable insights into its composition and properties. The analysis was carried out to assess the potential of eggshell waste as a sorbent material for its effectiveness in the removal process. The proximate analysis of eggshell bio-sorbent in this study typically involved the determination of the following parameters.

i. **Determination of moisture Content**:

The moisture content of the eggshell bio-sorbent was determined using the oven-drying method, following ASTM D2867-91 standards. In this method, 8 g of chicken eggshell powder was precisely weighed and placed in a high-temperature drying oven [10]. The samples were dried for a total of 3 h at a temperature of 105 °C. During the drying process, the weight of the samples was monitored at regular intervals of 30 min until a constant weight was obtained. This ensured that all the moisture within the samples was effectively removed by the drying process. The moisture content (MC) was determined using Equation (4) below. By employing the oven-drying method and applying Equation (4), the moisture content was accurately determined.

$$\%\ \text{Moisture content (MC)} = \frac{C-D}{C-B}x100 \tag{4}$$

Where B is the weight of the crucible, C is the weight of the crucible and sample before drying; and D is the weight of the crucible and sample after drying.

ii Determination of ash Content:

The ash content in the eggshell bio-sorbent was determined following the ASTM D2866-94 standard method. Ash content refers to the mineral matter that remains after the testing substance has been completely burned, representing the inorganic composition of the bio-sorbent. To determine the ash content, a crucible was first washed and dried in a hot air oven at a temperature of 550 °C for 30 min. After drying, the crucible was cooled in a desiccator for 30 min to ensure its stabilization. The crucible was then weighed using an analytical balance, and the initial weight (B) was recorded. Next, 8 g of the eggshell sample was accurately weighed into the crucible, and the combined weight (C) of the crucible and sample was recorded. The crucible with the sample was placed in a muffle furnace and heated at 550 °C for 3 h. After the heating process, the crucible with the resulting ash was cooled to room temperature, and its weight (D) was recorded after drying. This heating, cooling, and weighing process was repeated until a constant weight was achieved, indicating that all combustible materials were eliminated, and only the incombustible ash remained [21]. The ash content (AC) was determined using Equation (5).

$$\%\ \text{Ash content (AC)} = \frac{D-B}{C-B}x100 \tag{5}$$

Where B represents the weight of the crucible, C represents the weight of the crucible and sample before firing, and D represents the weight of the crucible and sample after firing.

iii. Determination of bulk density (ρB):

The bulk density (ρB) was determined following the ASTM D2854-96 standard method. It involved calculating the ratio of the mass of the adsorbent (mA) to the total volume (VT) of the cylinder, which consisted of the volume of the solid (VA) and any liquid present (VL). To have the experiment, 8 g of powdered eggshell and calcined CaO particles were placed in a graduated cylinder containing 100 ml. The volume occupied by the solid sample was recorded. This process was repeated twice, and the average value was taken. The bulk density for the sample was determined using Equation (6).

$$\text{Bulk density } (\rho\text{B}) = \frac{\textit{weight of dry sample}}{\textit{volume of packed sample in cubic centimeter}}$$

$$\rho\text{B} = \frac{MA}{VT} = \frac{MA}{V2+VA} \tag{6}$$

2.2.5. Characterization of the adsorbents: instrumental analysis

2.2.5.1. Fourier-transform infrared spectroscopy (FT-IR). To analyze the surface of the adsorbent composed of raw eggshells, corncob, and CaO NPs, an FTIR investigation was carried out. The PerkinElmer Spectrum 65 FT-IR model was utilized, operating at 4 cm^{-1} resolution in the range of 4000–400 cm-1. To make the Corncob-supported CaO NPs compatible with infrared analysis and obtain well-formed pellets, a small portion of the powdered eggshell sample was mixed with potassium bromide (KBr), an infrared-transparent matrix material. The mixture was ground and compressed under high pressure to form thin, uniform pellets. The prepared pellets were carefully placed on the sample holder, ensuring a smooth and even surface for measurement. The FTIR spectra were collected using a Fourier transform infrared spectrometer equipped with appropriate accessories. The pellet preparation technique allowed for efficient analysis, generating reliable and reproducible FTIR spectra.

2.2.5.2. X-ray diffraction (XRD) analysis. X-ray diffraction (XRD) analysis is a technique used in material science and engineering to determine the crystallographic structure of a material. It was also carried out to know the size of single-crystal CaO nanoparticles [22]. XRD analysis was performed using an analytical apparatus equipped with mono achromatized function at 40 KV and a current of 15 mA with Cuα radiation (λ = 0.154060 nm) and the sample was analyzed using a double crystal wide angle geometry with the 2θ scan from 10-90°. The XRD is used to determine the structural properties, to identify crystalline phase and orientation, how the atoms pack together in the crystalline state (atomic arrangement), and what the angle and interatomic distance are, etc [23,24]. Therefore, X-ray diffraction has become an essential and powerful tool for structural characterization in solid-state substances.

2.2.5.3. Thermal gravimetric analysis (TGA). Thermogravimetric analysis (TGA) is one of the most widely used thermal analysis methods. It is based on measuring the weight (mass) loss of solid materials as a function of temperature [25,26]. Using this, the decomposition temperature of raw eggshell powder, calcium hydroxide, and CaO particles was analyzed using a platinum crucible from ambient temperature to 1000 °C with a heating rate of 10 °C/min [27]. Thermal properties were observed by using TGA. The TGA

curve was used to determine the weight loss of the material. The loss of mass (weight) was due to decomposition, evaporation, reduction, and desorption.

2.2.5.4. Specific surface area. The specific surface area of hen eggshell powder and synthesized CaO NPs was determined using the Sears method [28]. One gram of adsorbent was mixed with 100 ml of distilled water and 20 gm of sodium chloride. The mixture was shaken for 5 min. Its final pH was adjusted to be 4 with 0.1 M hydrochloric acid and the volume at this pH was noted. It was then titrated with 0.1 M sodium hydroxide to increase the pH from 4 to 9. The volume (ml) of 0.1 M sodium hydroxide used was measured repeatedly, and the average value was used for calculating the specific surface area using the Sears method. The specific surface area of the adsorbent was calculated using the formula Sears method of [29] as indicated in Equation (7) below:

$$S = 32 * v - 25 \tag{7}$$

Where S is the surface area of the adsorbent per gram (m^2/g), V is the volume (ml) of 0.1 M sodium hydroxide required to raise the pH of the sample from 4 to 9. The numbers 32 and 25 are just physical constants.

2.2.6. Preparation of adsorbate

The wastewater contains various pollutants, including dyes, organic compounds, soluble and insoluble substances, and other metal ions [30]. So, it was very difficult to control at the laboratory to treat or separate these pollutants. In this case, studying the effect of cadmium (Cd^{2+}) metal ions on Nano CaO alone was appropriate. To avoid the disturbances of other soluble substances occurring in regular tap or drinking water, distilled water was used to dissolve the metal crystals. Cadmium acetate was helping as the source of the cadmium stock solution [31]. All the necessary solutions were prepared using analytical reagents and deionized water $C_4H_6CdO_4$ was used to give a clear colorless cadmium solution. A cadmium stock solution with (1000 mg/L) was prepared by dissolving 1.6146 g of 99% $C_4H_6CdO_4$ within 1 L of distilled water to prepare synthetic Cd^{2+} solution as a model pollutant and this was also used to prepare the working solutions with different initial Cadmium concentrations by taking different dilution amounts.

2.2.7. Batch adsorption experimental set-up

Batch adsorption experiments were set to investigate the removal of Cd^{2+} ions. Conical flasks with a 250 mL capacity were utilized for all experiments. In each experiment, the solution volume was 100 mL. The mixture of solution and the adsorbent was agitated by using a magnetic stirrer on a hot plate at 250 rpm. The initial solution pH was adjusted using a pH meter by dropping 0.1 M HCl or 0.1 M NaOH before adding the adsorbent to the solution. The temperature of the process was adjusted ambient on a hot plate and initial Cd (II) ion concentration was taken from synthetic Cd^{2+} ion solution by measuring cylinder. After the completion of the experimental set-up, the adsorption process started to take place. In this process, the Cd^{2+} ions in the solution interacted with the CaO nanoparticles, captivated by the attractive forces of the adsorbent surface. The unique physical and chemical properties of the adsorbent facilitated a strong affinity for Cd^{2+} ions. Consequently, the Cd^{2+} ions transferred from the solution to the surface of the adsorbent nanoparticles. This adsorption process continued until equilibrium was reached or a specific period was completed. After the batch adsorption process was completed, the samples underwent filtration utilizing What-man filter papers. Subsequently, the liquid fraction above the solid residue was subjected to analysis using a UV–visible spectrophotometer to determine the presence of Cd^{2+} ions. To explore the influence of dosage and initial concentration on the adsorption efficiency, each experiment was performed according to the experimental design layout. Various quantities of CaO nanoparticles were employed, along with different initial concentrations of Cd (II) solutions. This approach allowed for an examination of how changes in dosage and initial concentration impacted the overall adsorption efficiency. Fig. 2 illustrates a schematic of the batch adsorption experiment.

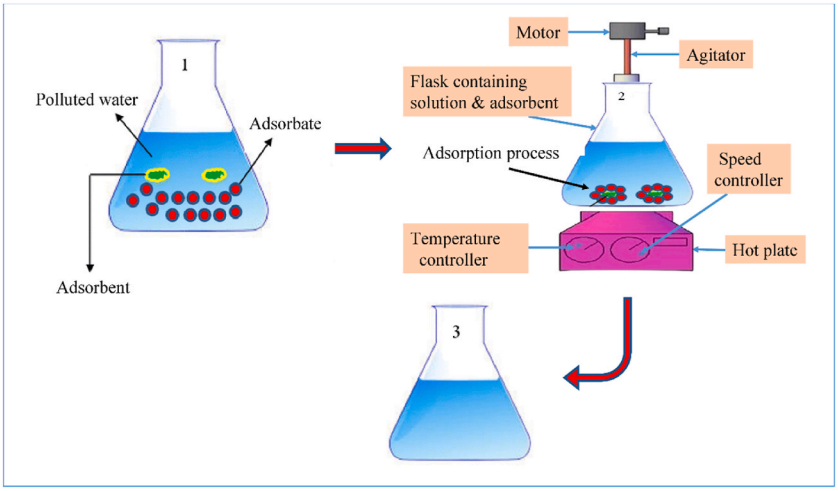

Fig. 2. Schematic of Batch Adsorption Experiment: (1) Polluted water, (2) Experimental set-up, (3) Unpolluted water.

The amount of contaminant adsorbed onto the unit weight of the adsorbent at equilibrium was calculated based on mass balance equations given by Equation (8) shown below & (Annane et al., 2021):

$$q = \frac{V(Co - Ce)}{m} \tag{8}$$

The removal efficiency (RE) of the adsorbent was obtained using Equation (9) shown below.

$$\%\ \text{Removal}\ (\text{R}) = \frac{Co - Ce}{Co} x100 \tag{9}$$

Where q represents the number of metal ions removed per gram of adsorbent, V (L) is the volume of the aqueous solution containing metal ions, C_0 (mg/L) is the initial amount of metal ions loaded, Ce (mg/L) is the amount of metal ion at equilibrium, and m (g) is the mass of adsorbent. To determine the equilibrium time, the percentage removal was observed at different contact times for each adsorbate. The experiment involved varying the loading of metal ions in the solutions from 15 mg/L to 95 mg/L. Furthermore, the effects of pH, achieved by using 0.1 M NaOH and 0.1 M HCl solutions, the dosage of adsorbent ranging from 0.5/100 ml g to 1.25 g/100 ml, contact time ranging from 15 min to 90 min, agitated speed at 250 rpm and initial adsorbate loading were investigated.

3. Results and discussions

3.1. Characterization of adsorbent

3.1.1. Proximate analysis

Proximate analysis was performed for raw eggshell and CaO particle adsorbent to analyze the physicochemical characteristics such as moisture content and ash content [32]. In this case, it provides information about the composition of raw egg shells and the resulting CaO particle adsorbent.

3.1.1.1. Moisture content. The moisture content percentages of the raw eggshells and CaO particles used as adsorbents were determined to be 0.98% and 0.135%, respectively. These values indicate that both raw eggshell and CaO particles have a lower moisture content compared to the 1.174% value reported in the literature [13]. CaO NPs, on the other hand, had a far longer shelf life than raw eggshell powder and were very stable, good-quality products [9]. The lower moisture content of the adsorbents is beneficial as it reduces the occupation of active sites by water, thereby increasing the maximum efficiency of adsorption before the adsorbent comes into contact with the solution [21]. Consequently, the adsorbents' ability to efficiently adsorb Cd (II) is improved, making them highly suitable for the intended application.

3.1.1.2. Ash content. The ash content of the eggshell samples was found to be 78.2% and 99.06% for raw eggshell and CaO particles, respectively. These values indicate a high inorganic substituent content in the eggshells. Comparing these results to other studies on the ash content of hen eggshells, it is evident that the ash content in this study was higher than the 45.29% reported in the previous literature [33]. This suggests that the CaO particle adsorbent derived from eggshells has a higher quality in terms of its inorganic content [28,34]. The findings align with the research conducted by Ref. [21], which also emphasized the positive correlation between ash content and removal efficiency. Therefore, the high ash content observed in the CaO particle adsorbent derived from eggshells suggests its potential as an effective adsorbent for achieving higher removal efficiencies.

Table 1 presents the results of the proximate analysis for raw egg shells and CaO particle adsorbent. These results from Table 1 provided insights into the composition and properties of raw egg shells and the resulting CaO particle adsorbent [12,35]. The differences in moisture content and ash content between the two materials highlight the transformation that occurs during the synthesis process. These findings can be valuable for understanding the characteristics and potential applications of the CaO particle adsorbent.

3.1.1.3. Particle density, bulk density, and porosity. Laboratory results of particle densities for both raw eggshell and CaO nanoparticles were 0.98 g/cm^3 and 2.00 g/cm^3 respectively. The results indicated that the particle density of calcium oxide nanoparticles was higher than that of the raw eggshell powders. This higher particle density resulted in increased porosity of the adsorbent. The measured bulk densities of the raw eggshell and calcium oxide nanoparticles were 0.623 g/cm^3 and 0.320 g/cm^3 respectively. These values were found to be lower than the reported bulk densities of raw eggshell (0.719 g/cm^3) and calcium oxide nanoparticles (0.375 g/cm^3) according to a study by Ref. [12]. The results of the adsorbent tests demonstrated that the particle density increased from raw eggshell to CaO nanoparticles, while the bulk density decreased. Based on these findings, it can be concluded that the lower bulk density of CaO nanoparticles, compared to its bulk materials, resulted in a higher porosity of the adsorbent.

Table 1
Results of proximate analysis.

Parameter	Raw egg shells	CaO particles Adsorbent
Moisture Content (%)	0.98	0.135
Ash Content (%)	78.2	99.06

According to the calculations of particle density and bulk density mentioned above, the porosity of raw eggshell and CaO NPs was 36.43 % and 81.34%, respectively. The porosity was calculated by subtracting the bulk density from the particle density, dividing the result by the particle density, and multiplying by 100 [36]. According to research on biomass, there are linear correlations between porosity and adsorptive processes [37]. The higher the porosity of an adsorbent, the greater its potential for adsorbing the adsorbate [38]. Therefore, based on these findings, it can be concluded that the lower bulk density of CaO nanoparticles, compared to its bulk materials, resulted in a higher porosity of the adsorbent.

3.1.2. FT-IR analysis

FT-IR analysis was used to look into the potential interactions between cadmium ions and biological components during the reduction reaction. The FTIR spectra of raw eggshell, corncob, and corncob-supported CaO NPs were utilized to measure functional groups' bending and stretching vibrations. Fig. 3a displays the FT-IR analyses of raw eggshell and corncob, while Fig. 3b presents the FT-IR analyses of corncob-supported CaO NPs, both before and after the adsorption of Cd (II) ions. The spectral range covered in these analyses was 4000–400 cm^{-1}. The characteristic peaks of calcium carbonate in FT-IR spectra of the eggshell, as can be seen from Fig. 3a, appeared at 1600 cm^{-1}. The corncob nanoparticle has a large absorption peak at 1631 cm^{-1} that is related to the carbonyl group's C–O stretching [16].

The spectra of corncob-supported CaO NPs before and after the adsorption of Cd (II) ions exhibit similar bands. The uniformity of peaks observed can be attributed to the absorption of moisture and carbon dioxide from the surrounding environment [39]. A broad peak observed at 3420 cm^{-1} as shown in Fig. 3b is indicative of the presence of an O–H free hydroxyl bond, which likely originates from residual hydroxide [40]. Several other bands have also been observed at 1599 cm^{-1} (C–O bond due to carbonation), and around 2818 cm^{-1} (associated with CO_2 stretching and C–O stretch). These peaks align with the expected frequencies for C–O stretch vibrations [39,41,42]. A distinct peak at 625 cm^{-1} indicated the Ca–O bond stretch, which confirms the presence of CaO in the samples [43]. The absence of a sharp absorption in the area between 1075 cm^{-1} and 1130 cm^{-1} suggests that the $CaCO_3$ was no longer present in the sample since it had been changed into CaO [18]. In the spectrum of corncob-supported CaO NPs exposed to Cd (II) ions, a

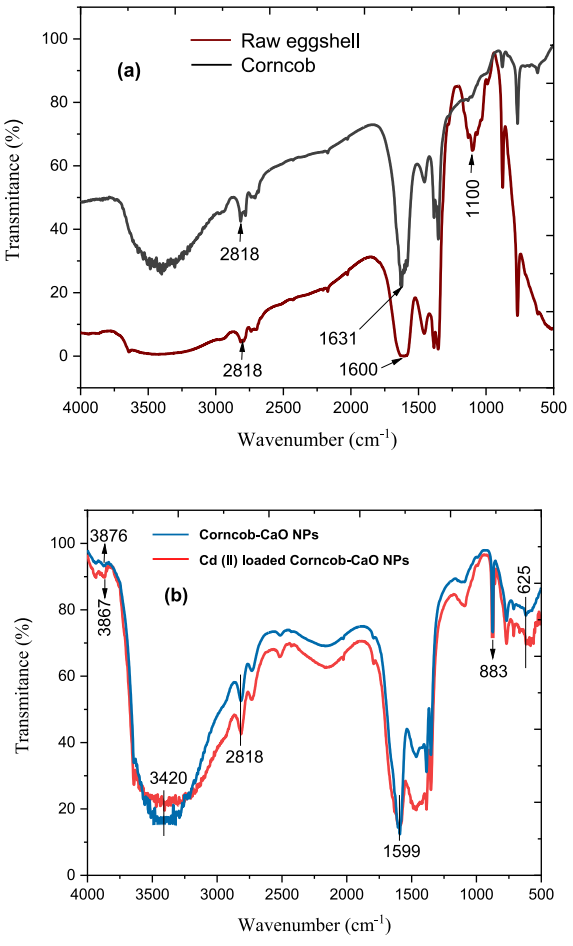

Fig. 3. FTIR spectra of: (a) Eggshell and Corncob (b) Corncob-CaO NPs and Cd (II) loaded Corncob-CaO NPs.

decrease in peak intensity and selective shifts or changes in wavenumbers were observed. These changes suggest the potential absorption of Cd (II) ions by the O–H, C–O, and Ca–O bonds, leading to alterations in peak frequencies [44,45]. These findings indicate the involvement of the adsorbent, corncob-supported CaO nanoparticles, in the adsorption process of Cd (II) ions.

Table 2 below depicts the main difference between the wavenumbers before and after Cd (II) adsorption process. The changes in the wavenumbers were small, less than 15 cm^{-1}. This result indicated the possibility that the adsorption process could take place via an ion exchange process or physical interaction [46].

3.1.3. X-ray diffraction (XRD) analysis

XRD analysis was conducted to investigate the crystal structure and crystallinity of the synthesized calcium oxide nanoparticles (CaO NPs) and corncob-based samples. With regards to the XRD pattern of the CaO NPs, as shown in Fig. 4a, prominent peaks were observed at specific 2θ angles, which strongly correlated with the Joint Crystal Powder Diffraction Standard (JCPDS) card number 77–2376. This finding confirms the presence of well-polycrystalline CaO nanoparticles. Notably, the peak at $2\theta = 37.51^{\circ}$ provided strong evidence for the presence of CaO nanoparticles. Additional peaks were observed at various 2θ angles, such as 29.17°, 32.35°, 33.79°, 48.43°, 54.01°, 64.3°, and 67.54°. The XRD peak profiles displayed sharpness and narrow spectral width, indicating a well-crystallized structure of the CaO NPs. However, we also noticed the presence of impure phase peaks, potentially $Ca(OH)_2$, implying the existence of moisture in the synthesized nanoparticles, likely attributed to the oxidation of CaO during the nanoparticle synthesis process and subsequent exposure to the environment. Moreover, to determine the mean crystallite size of the CaO NPs, we employed Scherer's Equation as described in the study [47]. Equation (10) shows Scherer's Equation.

$$d = \frac{k\lambda}{\beta \cos \theta} \tag{10}$$

Where *d* is the mean crystallite size, λ is the wavelength, k is the constant of Scherrer, θ is Bragg's angle and β is the FWHM of the peak. Based on this analysis, the average crystallite size of the CaO nanoparticles was determined to be 24.34 nm. This result indicates that the synthesized nanoparticles exhibit a nanocrystalline structure, with relatively larger crystallite size. This finding of larger crystallite is consistent with the results reported by other researchers who employed the sol-gel method for nanoparticle synthesis [34,39,48].

For the corncob-based samples, the XRD pattern, as displayed in Fig. 4b, also exhibited distinct peaks at specific 2θ angles, indicating the presence of crystalline phases. The peaks were labeled and associated with their respective crystallographic planes. Notably, the peaks at $2\theta = 23.41^{\circ}$, 30.48°, 35.53°, 57.52°, and 63.13° were clearly identified. The corresponding d-spacings were calculated using Bragg's Law, Equation (11) below, and found to be 3.796 Å, 2.929 Å, 2.524 Å, 1.6 Å, and 1.47 Å, respectively.

$$n\lambda = 2d \sin(\theta) \tag{11}$$

Where n is the order of the reflection, λ is the wavelength of the X-ray, d is the spacing between crystal lattice planes, and θ is the angle between the incident X-ray beam and the crystal lattice planes.

Furthermore, the XRD analysis allowed for the estimation of the average crystallite size of the corncob-based nanoparticles. The peaks at $2\theta = 37.221^{\circ}$ and 34.787° were utilized for this purpose. Using Scherer's Equation and the full width at half maximum (FWHM) of the peaks, the average crystallite size was determined to be approximately 16 nm and 33 nm, respectively. These findings are consistent with the results reported by Ref. [49].

3.1.4. Thermogravimetric Analysis

Thermogravimetric Analysis (TGA) was performed to evaluate the decomposition behavior of CaO nanoparticles (NPs) and corncob. The TGA curves provided insights into the weight loss stages and thermal stability of the samples. In the $Ca(OH)_2$ gel derived from hen eggshell powder, three distinct weight-loss stages were observed, as depicted in Fig. 5 (b). The first stage, occurring between temperatures of 45.14 °C and 432.05 °C, involved the vaporization of adsorbed water, resulting in a weight loss of 89.4564%. The second stage, within the temperature range of 174.18 °C–669.40 °C, corresponded to the decomposition of the gel $Ca(OH)_2$ into CaO, causing a mass loss of 75.99%. The final stage involved the breakdown of $CaCO_3$ into CaO and the release of carbon dioxide, resulting in a mass loss of 44.6% between temperatures of 631.32 °C and 865.6 °C. Above 865.6 °C, the gel exhibited stability and did not significantly lose weight. The total weight loss until 865.6 °C was 80.4%. Additionally, the CaO NP adsorbent experienced only a minor weight loss of 4.7% between temperatures of 356 °C and 385 °C, which can be attributed to the loss of CO_2 during the carbonization of CaO. This TGA analysis confirmed the excellent thermal stability and purity of CaO nanoparticles. Comparable results have been

Table 2
FT-IR spectral characteristics of CaO NPs before and after Cd (II) ion adsorption.

Functional group of FTIR absorption bands	Wave number cm^{-1} Adsorption band		
	Before Adsorption Cd (II)	After Adsorption	Shift difference
OH, hydroxyl	3876	3867	11
C═C, Alkenes	3441	3437	4
C, symmetric	2818	2817	1
C═O, Carbonyl	1599	1588	11
Carboxylic Acid	883	877	6

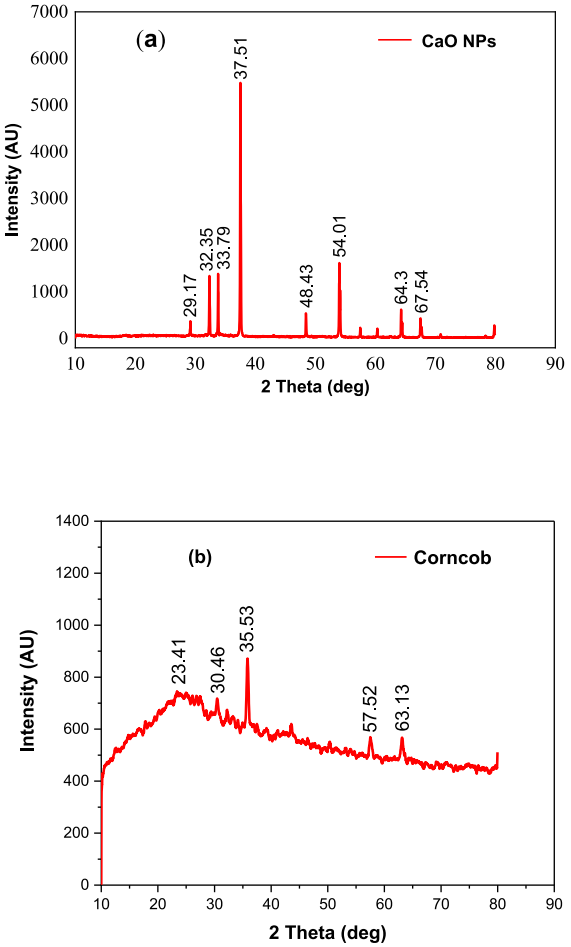

Fig. 4. XRD graph of (a) Eggshell Calcium Oxide Nanoparticles and (b) Corncob.

reported by Refs. [9,12].

The TGA curves for corncob pyrolysis, depicted in Fig. 5 (a), revealed characteristic weight-loss stages. In non-catalytic runs, a major weight-loss stage occurred in the temperature range of approximately 32.5 °C–433.50 °C. However, in catalytic runs with corncob, three major weight-loss stages were observed. The first stage exhibited a weight loss of 32.2% between 100 °C and 116 °C. The second stage involved a weight loss of 16.70% between 200 °C and 320 °C. The third stage (III) displayed a weight loss of 12.38% between 320 °C and 433.3 °C. The decomposition of cellulose primarily occurred between 275 °C and 350 °C, while hemicellulose decomposed mainly between 150 °C and 350 °C. This finding aligns with the results obtained by Ref. [50].

3.1.5. Determination of specific surface area

As stated in the material and method section, the surface area was calculated using equation (8). This technique can yield CA with a specific surface area of s = 2700 m^2/g. Pre-carbonizing the corncob in a sealed ceramic oven at 450 °C for 1.5 h, followed by chemical activation with KOH at 780 °C and CO_2 gasification, resulted in CA with a significant specific surface area. CaO NPs have a surface area of 77.4 m^2/g. Between 60 and 90 m^2/g was the reported specific surface area. This titration experiment produces nanoparticle adsorbents, which increase the specific surface area of the adsorbents through the calcination process [51,52]. The adsorbent's specific surface area increases with improved adsorption capability [29,53].

3.2. Cd (II) absorption studies

At the end of the lead absorption study, the residual/suspension was separated through filtration processes. All 30 run experiments were done with a different combination of four parameters and the values were recorded as illustrated in Table 3.

The investigation adsorption process of Cd (II) on calcium oxide nanoparticle characterizations has been discussed considering the effect of individual factors.

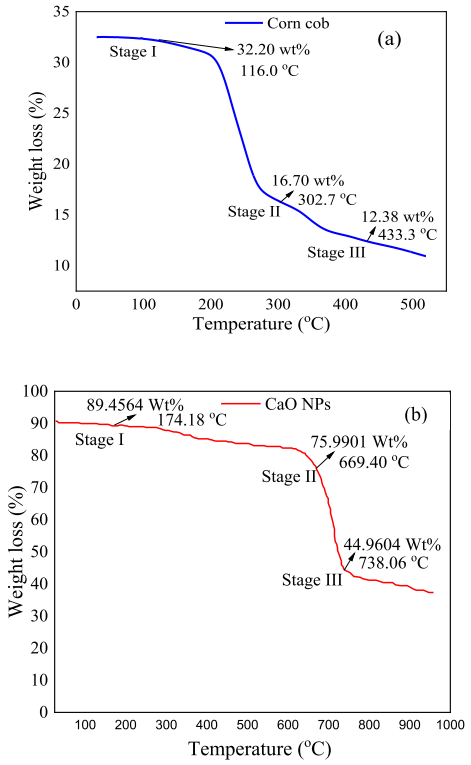

Fig. 5. TGA graph of Corncob (a) and Calcium Oxides Nanoparticle (b).

3.2.1. *Effect of pH on Cd (II) removal*

The adsorption of Cd (II) ions from aqueous solution using CaO nanoparticles was dependent on the pH of the solution used in this study. At pH values higher than the point of zero charge (PZC) of CaO, the surface of the nanoparticles becomes negatively charged, which favors the adsorption of positively charged Cd (II) ions. As a result, the percentage of Cd (II) ions removed increases with increasing pH as shown in Fig. 6. At pH 3, the removal efficiency of Cd (II) was 85.3252%, while at pH 7, the removal efficiency was 99.1084%. This was because there were fewer H^+ ions in the solution at higher pH values that reduced competition with Cd (II) ions for adsorption sites. Additionally, the higher pH favors the deprotonation of surface functional groups on the CaO nanoparticles, which created more negatively charged sites for Cd (II) ion adsorption. At pH values lower than the PZC of CaO, the surface of the nanoparticles becomes positively charged. This leads to repulsion between the positively charged CaO nanoparticles and the positively charged Cd (II) ions, which reduces the removal efficiency of Cd (II). In alkaline conditions (pH greater than 7), the removal efficiency of Cd (II) decreases. This was because the formation of hydroxyl ions (OH^-) at high pH values could compete with Cd (II) ions for adsorption sites on the CaO nanoparticles. Additionally, the high pH can lead to the precipitation of Cd (II) as cadmium hydroxide, which reduces the amount of Cd (II) in solution that was available for adsorption. As a result, the pH of the solution had a significant impact on the removal of Cd (II) ions using CaO nanoparticles. The highest removal efficiency was achieved at pH values higher than the PZC of CaO, where the surface of the nanoparticles was negatively charged and there was less competition from H^+ ions for adsorption sites and these findings align with a similar result reported in the literature by Ref. [53]. Fig. 6 below shows the effect of pH on Cadmium (II) removal from aqueous solution.

3.2.2. *Effect of adsorbent dosage*

The study investigated the impact of varying the dosage of CaO nanoparticles (NPs) (comprising 85% CaO NPs and 15% Corncob sample) on the adsorption of Cd (II) ions in an aqueous solution. The dosage range was varied from 0.25 g to 1.25 g while keeping the initial concentration, solution pH, and contact time constant. The results revealed that the removal efficiency of Cd (II) ions increased with higher dosages of CaO NPs. This can be attributed to the increased availability of adsorptive (binding) sites and a larger surface area provided by the higher amount of CaO NPs. Consequently, Cd (II) removal efficiency improved, particularly at a neutral pH, 50 min of contact time, and an initial concentration of 55 g/ml of Cd (II) ions. At a dosage of 0.25 g/100 ml, the percentage of Cd (II) removal from the aqueous solution using CaO NPs and Corncob rapidly reached 97.133%. Subsequently, at a dosage of 0.75 g/100 ml, the removal efficiency of Cd (II) increased slowly, reaching a value of 99.1084%. However, beyond the optimal dosage, further increases in the adsorbent dosage did not lead to a significant improvement in the removal of Cadmium (II). It is worth noting that although the dosage of CaO NPs and Corncob increased, the corresponding increase in Cd elimination was not proportional. The

Table 3
Experimental results of Cd (II) adsorption experiments.

Run	pH	Contact time (min)	Dosage (g/)	Concentration (mg/L)	Absorbance	Ce Final conc.	Removal Efficiency%
1	5	30	0.5	35	0.004	2.1192	93.9451
2	5	70	1	35	0.005	1.7954	94.8703
3	9	30	0.5	35	0.0011	1.8404	94.7418
4	5	30	1	35	0.0024	2.4554	92.9846
5	7	50	0.75	55	0.0013	0.7396	98.6552
6	9	70	1	35	0.034	1.1538	96.7033
7	7	50	0.75	55	0.00012	0.7362	98.6615
8	9	70	1	75	0.011	3.0423	95.9436
9	5	30	1	75	0.082	6.6442	91.1411
10	5	70	1	75	0.072	5.3077	92.9231
11	11	50	0.75	55	0.045	5.7115	89.6154
12	9	70	0.5	75	0.01	2.9462	96.0718
13	5	70	0.5	75	0.019	5.3116	92.9179
14	7	50	0.75	55	0.0015	0.8138	98.5203
15	7	90	0.75	55	0.004	2.3192	95.7832
16	7	50	0.75	55	0.002	0.7519	98.6329
17	9	30	0.5	75	0.002	3.3769	95.4974
18	5	70	0.5	35	0.011	2.2323	93.6221
19	7	10	0.75	55	0.003	3.3780	93.8581
20	7	50	0.75	55	0.005	0.7104	98.7084
21	7	50	0.75	15	0.006	0.1465	99.0231
22	7	50	1.25	55	0.0017	1.7571	96.8053
23	7	50	0.75	55	0.005	0.4904	99.1084
24	9	30	1	35	0.006	1.9615	94.3956
25	5	30	0.5	75	0.011	5.4423	92.7436
26	9	30	1	75	0.034	4.6538	93.7949
27	7	50	0.25	55	0.006	1.5765	97.1336
28	3	50	0.75	55	0.0867	8.0711	85.325
29	9	70	0.5	35	0.0036	1.7307	95.0549
30	7	50	0.75	95	0.008	1.951	97.946

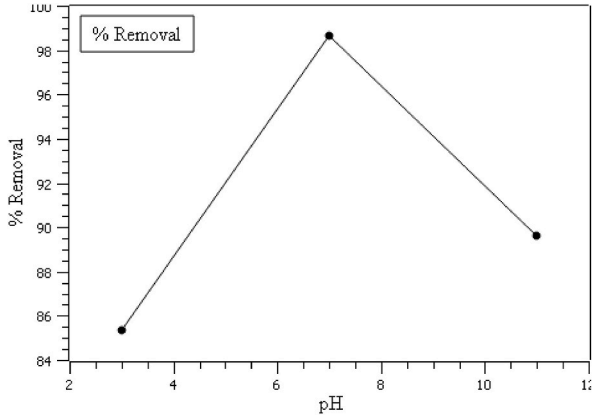

Fig. 6. Effect of pH on Cadmium (II) removal.

removal efficiency at 1 g/L dosage was not as high as that at 5 g/L dosage. Additionally, at pH 7, there was an incremental increase in the differential of bio-sorption capacity by 25 mg/L and removal efficiency by 6 percent and these findings align with a similar result reported in the literature by Ref. [28]. The findings underscore the importance of optimizing the dosage of CaO NPs in Cd (II) ion adsorption processes, taking into account the maximum removal efficiency achieved at the optimal dosage without exceeding it. The effect of adsorbent dosage on Cd (II) removal is shown in Fig. 7 below.

3.2.3. Effect of contact time

Contact time was an important factor in determining the adsorption of Cd (II) ions onto CaO nanoparticles. The effect of contact times (from 10 to 90min) of the removal of Cd (II) was shown in Fig. 8. At the beginning of the adsorption process, the concentration of Cd (II) ions in the solution is high and there are many available adsorption sites on the CaO nanoparticles. As a result, the amount of Cd (II) ions removed and the adsorption capacity increase rapidly with increasing contact time. After about 50 min, the concentration of Cd (II) ions in the solution decreases and the available adsorption sites on the CaO nanoparticles become limited. As a result, the

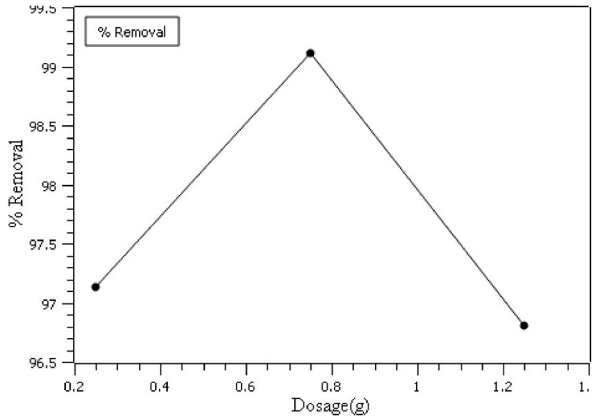

Fig. 7. Effect of adsorbent dosage on Cd (II) removal.

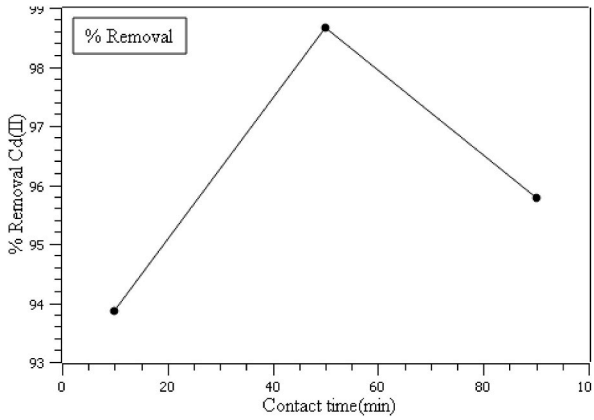

Fig. 8. Effect of contact time on Cd (II) removal.

adsorption process slows down and eventually reaches equilibrium. Increasing the contact time beyond this point does not significantly increase the amount of Cd (II) ions removed or the adsorption capacity. This is consistent with the findings of [21] who reported that the amount of cadmium that can be adsorbed at equilibrium increases with a decrease in adsorbent size. This is because smaller adsorbent particles have a larger surface area, which provides more adsorption sites for Cd (II) ions. Therefore, the contact time required for the adsorption of Cd (II) ions onto CaO nanoparticles depends on the initial concentration of Cd (II) ions in the solution and the size of the CaO nanoparticles. Once equilibrium is reached, increasing the contact time does not significantly increase the amount of Cd (II) ions removed or the adsorption capacity.

3.2.4. Effect of initial metal concentration

The impact of the initial metal concentration on adsorption was investigated, as shown in Fig. 9. The study examined the effects of varying Cd (II) concentrations, ranging from 15 to 95 g/ml while keeping the adsorbent dose, solution pH, and contact time fixed at 0.75 g, 7, and 50 min, respectively. The results indicate that as the initial concentration of Cd (II) increased, the removal percentage of Cd (II) decreased. At an initial concentration of 15 g/ml, the efficiency of removing cadmium (II) was 99.0231 percent, while at an initial concentration of 95 g/ml, it was 97.946 percent. This decrease in removal efficiency can be attributed to a limited number of active sites on the adsorbent surface. As the concentrations of Cd (II) increase, the available binding sites become less abundant compared to the metal ions, resulting in a lower clearance percentage. This observation indicates the saturation of active sites on CaO NP samples for interacting with contaminants, suggesting that as concentrations increase, the process becomes less favorable in terms of available sites. However, it is important to note that the interaction between Cd (II) and CaO NPs intensifies with increasing initial Cd (II) concentrations, leading to enhanced Cd adsorption. This is due to the increased driving force resulting from the concentration gradient when both Cd (II) ions and adsorbent material concentrations rise. Consequently, the rate of adsorption (removal percentage) and metal uptake decreased as the concentration of Cd (II) increased.

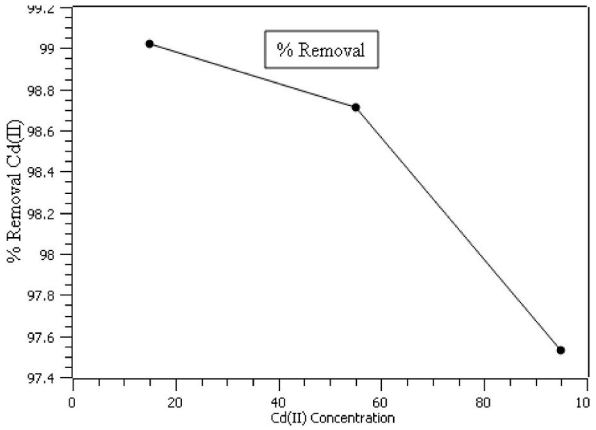

Fig. 9. Effect of initial concentration on Cadmium (II) adsorption.

4. Conclusions

In this study, calcium oxide nanoparticles (CaO NPs) synthesized from waste hen eggshells using a sol-gel method and supported on corncob bio-adsorbent were effectively utilized to remove cadmium ions from aqueous solutions. The synthesized CaO NPs were characterized using FT-IR, XRD, specific surface area, and TGA. Batch adsorption experiments were conducted to systematically investigate the influence of key process parameters, including adsorbent dosages, initial Cd (II) concentrations, pH values, and contact times. By optimizing these conditions, it was determined that the highest percent removal of cadmium (99.108%) could be achieved with an initial concentration of 55 ppm, pH 7, adsorbent dose of 0.75 g, and contact time of 50 min. The experimental removal efficiency closely matched the predicted value (99.0%), validating the effectiveness of the applied method for optimizing the removal of Cd (II) ions from aqueous solutions. The utilization of waste hen eggshells as a precursor for the synthesis of CaO NPs adds to the sustainability of the process. Additionally, the corncob bio-adsorbent is a renewable and low-cost material, making the overall process even more cost-effective and environmentally friendly. Based on these findings, the corncob-supported CaO NPs can be considered a promising and sustainable adsorbent for the removal of cadmium ions from wastewater. Further studies are required to evaluate the performance of the adsorbent in real wastewater matrices and to develop scalable and cost-effective regeneration methods.

Funding

This work was financially supported by Jimma University, Jimma Institute of Technology.

Data availability statement

All data are available within the manuscript.

CRediT authorship contribution statement

Werkne Sorsa Muleta: Writing – original draft, Funding acquisition. **Sultan Mulisa Denboba:** Investigation, Data curation. **Abreham Bekele Bayu:** Writing – review & editing, Supervision, Project administration.

Declaration of competing interest

The authors declare the following financial interests/personal relationships which may be considered as potential competing interests:Werkne Sorsa Muleta reports financial support was provided by Jimma University Institute of Technology. Sultan Mulisa Denboba reports a relationship with Jimma University Institute of Technology that includes: employment. Abreham Bekele Bayu has patent NA pending to NA. All of authors are academic staffs in Jimma Institute of Technology, Ethiopia If there are other authors, they declare that they have no known competing financial interests or personal relationships that could have appeared to influence the work reported in this paper.

Acknowledgment

Special acknowledgment goes to the School of Chemical Engineering laboratory and the Faculty of Materials Science and Engineering Laboratory at Jimma Institute of Technology for generously granting us access to all the resources available in their laboratories.

References

[1] O.G. Abatan, P.A. Alaba, B.A. Oni, K. Akpojevwe, V. Efeovbokhan, F. Abnisa, Performance of eggshell powder as an adsorbent for adsorption of hexavalent chromium and cadmium from wastewater, SN Appl. Sci. 2 (12) (2020) 1996, https://doi.org/10.1007/s42452-020-03866-w.

[2] F. Carolin, P. Kumar, S. Anbalagan, J. Joshiba, M. Naushad, Efficient techniques for the removal of toxic heavy metals from aquatic environment: a review, J. Environ. Chem. Eng. 5 (2017), https://doi.org/10.1016/j.jece.2017.05.029.

[3] F. Ajala, A. Hamrouni, A. Houas, H. Lachheb, B. Megna, L. Palmisano, F. Parrino, The influence of Al doping on the photocatalytic activity of nanostructured ZnO: the role of adsorbed water, Appl. Surf. Sci. 445 (2018), https://doi.org/10.1016/j.apsusc.2018.03.141.

[4] H. Norouzi, D. Jafari, M. Esfandyari, Study on a new adsorbent for biosorption of cadmium ion from aqueous solution by activated carbon prepared from Ricinus communis, Desal. Water Treat 191 (2020) 140–152, https://doi.org/10.5004/dwt.2020.25702.

[5] A. Khedri, D. Jafari, M. Esfandyari, Adsorption of nickel (II) ions from synthetic wastewater using activated carbon prepared from Mespilus germanica Leaf, Arabian J. Sci. Eng. (2021) 1–12, https://doi.org/10.1007/s13369-021-06014-7.

[6] A.A. Behroozpour, D. Jafari, M. Esfandyari, S.A. Jafari, Prediction of the continuous cadmium removal efficiency from aqueous solution by the packed-bed column using GMDH and ANFIS models, Desalination Water Treat. 234 (2021) 91–101, https://doi.org/10.5004/dwt.2021.27591.

[7] S. Rajendran, P. Ak, P. Kumar, T. Hoang, K. Sekar, K.Y. Chong, K.S. Khoo, H.S. Ng, P.-L. Show, Critical and recent developments on adsorption technique for removal of heavy metals from wastewater-A review, Chemosphere 303 (2022) 135146, https://doi.org/10.1016/j.chemosphere.2022.135146.

[8] C. Grégorio, E. Lichtfouse, L. Wilson, N. Crini, Conventional and non-conventional adsorbents for wastewater treatment, Environ. Chem. Lett. 17 (2018), https://doi.org/10.1007/s10311-018-0786-8.

[9] R. Jalu, T. Ayala, R. Kasirajan, Calcium oxide nanoparticles synthesis from hen eggshells for removal of lead (Pb(II)) from aqueous solution, Environmental Challenges 4 (2021) 100193, https://doi.org/10.1016/j.envc.2021.100193.

[10] T. Alslaibi, I. Abustan, M. Azmier, A. Foul, Cadmium removal from aqueous solution using microwaved olive stone activated carbon, J. Environ. Chem. Eng. 1 (2013) 589–599, https://doi.org/10.1016/j.jece.2013.06.028.

[11] P. Praipipat, P. Ngamsurach, R. Tannadee, Influence of duck eggshell powder modifications by the calcination process or addition of iron (III) oxide-hydroxide on lead removal efficiency, Sci. Rep. 13 (1) (2023) 12100, https://doi.org/10.1038/s41598-023-39325-w.

[12] R. Kasirajan, A. Bayu, J. Aklilu, Adsorption of Lead (Pb-II) using CaO-NPs synthesized by sol-gel process from hen eggshell: response Surface Methodology for modeling, optimization, and kinetic studies, S. Afr. J. Chem. Eng. 40 (2022) 209–229. https://hdl.handle.net/10520/ejc-chemeng-v40-n1-a19.

[13] A.B. Bayu, T. Abeto Amibo, S.M. Beyan, Adsorptive capacity of calcinated hen eggshell blended with silica gel for removal of lead II ions from aqueous media: kinetics and equilibrium studies, Journal of Environmental and Public Health 2022 (2022) 2882546, https://doi.org/10.1155/2022/2882546.

[14] P.I. Ali, V. Gupta, Advances in water treatment by adsorption Technology, Nat. Protoc. 1 (2006) 2661–2667, https://doi.org/10.1038/nprot.2006.370.

[15] H. Alhaj, S. Almabrok, M. El-Ajaily, REMOVAL OF CADMIUM(II) ION FROM AQUEOUS SOLUTIONS BY ORANGE PEELS, Global scientific Journals 7 (2) (2019). www.globalscientificjournal.com.

[16] S. Kumar, Y. Negi, J. Upadhyaya, Studies on characterization of corn cob based nanoparticles, Adv. Mater. Lett. 1 (2010), https://doi.org/10.5185/amlett.2010.9164.

[17] M. Pichhode, K. Nikhil, Effect of heavy metals on plants: an overview, Int. J. Appl. Innov. Eng. Manag. (IJAIEM) 5 (3) (2016). www.ijaiem.org.

[18] L. Habte, Synthesis of nano-calcium oxide from waste eggshell by sol-gel method, Sustainability 11 (2019), https://doi.org/10.3390/su11113196.

[19] E. Kianfar, W. Suksatan, Nanomaterial by sol-gel method: synthesis and application, Adv. Mater. Sci. Eng. 2021 (2021) 1–21, https://doi.org/10.1155/2021/5102014.

[20] R. Malik, D.S. Ramteke, S.R. Wate, Physico-chemical and surface characterization of adsorbent prepared from groundnut shell by ZnCl 2 activation and its ability to adsorb color, Indian J. Chem. Technol. 13 (2006). http://nopr.niscpr.res.in/handle/123456789/7048.

[21] S. Ayub, A. Mohammadi, M. Yousefi, F. Changani khorasgani, Performance evaluation of agro-based adsorbents for the removal of cadmium from wastewater, Desalination Water Treat. 142 (2019) 293–299, https://doi.org/10.5004/dwt.2019.23455.

[22] J. Epp, X-ray diffraction (XRD) Techniques for Materials Characterization (2016) 81–124, https://doi.org/10.1016/B978-0-08-100040-3.00004-3.

[23] MS. Shackley. X-ray fluorescence (XRF): applications in archaeology. InEncyclopedia of Global Archaeology, Springer International Publishing, Cham, 2020, pp. 11381–11387. https://doi.org/10.1007/978-3-030-30018-0_1305.

[24] K. Tashiro, Crystal Structure Analysis by Wide-Angle X-ray Diffraction Method (2022) 1–285, https://doi.org/10.1007/978-981-15-9562-2_1.

[25] R. Bernhoft, Cadmium toxicity and treatment, TheScientificWorldJOURNAL 2013 (2013) 394652, https://doi.org/10.1155/2013/394652.

[26] I. Alsurakji, A. El-Qanni, A. El-Hamouz, I. Warad, Y. Odeh, Thermogravimetric kinetics study of scrap tires pyrolysis using silica embedded with NiO and/or MgO nanocatalysts, J. Energy Resour. Technol. 143 (2021) 1–15, https://doi.org/10.1115/1.4050814.

[27] R. Bushra, M. Shahadat, A. Raeisssi, S. Nabi, Development of nano-composite adsorbent for removal of heavy metals from industrial effluent and synthetic mixtures; its conducting behavior, Desalination 289 (2012) 1–11, https://doi.org/10.1016/j.desal.2011.12.013.

[28] G. Chen, G. Zeng, L. Tang, C. Du, X. Jiang, G. Huang, H. Liu, G. Shen, Cadmium removal from simulated wastewater to biomass byproduct of lentinus edodes, Bioresour. Technol. 99 (2008) 7034–7040, https://doi.org/10.1016/j.biortech.2008.01.020.

[29] F. Heinroth, R. Münnekhoff, C. Panz, R. Schmoll, J. Behnisch, P. Behrens, The Sears number as a probe for the surface chemistry of porous silicas: precipitated, pyrogenic, and ordered mesoporous silicas, Microporous Mesoporous Mater. 116 (2008) 95–100, https://doi.org/10.1016/j.micromeso.2008.03.022.

[30] T.M.A. Shaikh, Adsorption of Pb(II) from wastewater by natural and synthetic adsorbents, Biointerface Research in Applied Chemistry 10 (2020) 6522–6539, https://doi.org/10.33263/BRIAC105.65226539.

[31] Y. Sun, J.P. Zhang, G. Yang, Z.H. Li, An improved process for preparing activated carbon with large specific surface area from corncob, Chem. Biochem.Eng. Q. 21 (2) (2007) 21, https://doi.org/10.22146/ijc.53057. cabeq@pbf.hr.

[32] N. Amjed, I. Bhatti, K. Arif, A. Nazir, M. Zahid, Variations in the physicochemical profile of khushab coal under various environmental conditions, Pol. J. Environ. Stud. 27 (2018). http://www.pjoes.com/pdf-70632-24321?filename=24321.pdf.

[33] O. Ajala, O. Eletta, M.A. Ajala, S. Oyeniyi, Charactrization and evaluation of chicken egg shell for use as bio-resource, Arid zone Journal of Engineering, Technology and Environment 14 (1) (2018) 26. www.azojete.com.ng.

[34] A. Younes, Y. Abdulhady, N. Shahat, F. El-Dars, Removal of cadmium ions from wastewaters using corn cobs supporting nano-zero valent iron, Separ. Sci. Technol. 56 (2019) 1–13, https://doi.org/10.1080/01496395.2019.1708109.

[35] W. Tsai, J.-m. Yang, C. Lai, Y.H. Cheng, C. Lin, C. Yeh, Characterization and adsorption properties of eggshells and eggshell membrane, Bioresour. Technol. 97 (2006) 488–493, https://doi.org/10.1016/j.biortech.2005.02.050.

[36] M. Ghaedi, Adsorption: Fundamental Processes and Applications, Academic Press, 2021, https://doi.org/10.1016/S0001-8686(00)00082-8.

[37] U. Garg, M. Kaur, G. Jawa, D. Sud, V.K. Garg, Removal of cadmium(II) from aqueous solutions by adsorption on agricultural waste biomass, J. Hazard Mater. 154 (2008) 1149–1157, https://doi.org/10.1016/j.jhazmat.2007.11.040.

[38] C.-T. Hsieh, H. Teng, Influence of mesopore volume and adsorbate size on adsorption capacities of activated carbons in aqueous solutions, Carbon 38 (2000) 863–869, https://doi.org/10.1016/S0008-6223(99)00180-3.

[39] L. Joseph, B.-M. Jun, J. Flora, C.M. Park, Y. Yoon, Removal of heavy metals from water sources in the developing world using low-cost materials: a review, Chemosphere 229 (2019), https://doi.org/10.1016/j.chemosphere.2019.04.198.

[40] D. Singh, R. Gautam, R. Kumar, B. Shukla, V. Shankar, V. Krishna, Citric acid-coated magnetic nanoparticles: synthesis, characterization, and application in removal of Cd(II) ions from aqueous solution, J. Water Proc. Eng. 4 (2014), https://doi.org/10.1016/j.jwpe.2014.10.005.

[41] T.A. Amibo, D. Konopacka-Łyskawa, The influence of α, ω-diols and SiO2 particles on CO2 absorption and NH3 escaping during carbon dioxide capture in ammonia solutions, J. CO2 Util. 80 (2024 Feb 1) 102698, https://doi.org/10.1016/j.jcou.2024.102698.

[42] D. Konopacka-Łyskawa, T. Abeto Amibo, D. Dobrzyniewski, M. Łapiński, Improving carbon dioxide capture in aqueous ammonia solutions by fine SiO 2 particles, Chem. Process Eng.: News Front. (2023), https://doi.org/10.24425/cpe.2023.146718.

[43] L. Correia, R. Saboya, N. Campelo, J.A. Cecilia, E. Rodriguez-Castellon, C. Cavalcante Jr., R. Vieira, Characterization of calcium oxide catalysts from natural sources and their application in the transesterification of sunflower oil, Bioresour. Technol. 151C (2013) 207–213, https://doi.org/10.1016/j.biortech.2013.10.046.
[44] E. Asuquo, A. Martin, P. Nzerem, F. Siperstein, X. Fan, Adsorption of Cd(II) and Pb(II) ions from aqueous solutions using mesoporous activated carbon adsorbent: equilibrium, kinetics, and characterization studies, J. Environ. Chem. Eng. 5 (2016), https://doi.org/10.1016/j.jece.2016.12.043.
[45] R. Shrestha, S. Joshi, Isotherms and kinetic studies on the adsorption of Cd(II) onto activated carbon prepared from coconut (cocos nucifera) shell, J. Nepal Chem. Soc. 40 (2019) 78–83, research/tech/periodicals/doi.php?art_seq=1020237.
[46] E. Elkhatib, A. Mahdy, F. Sherif, W. Elshemy, Competitive adsorption of cadmium (II) from aqueous solutions onto nanoparticles of water treatment residual, Journal of Nanomaterials 2016 (2016) 8496798, https://doi.org/10.1155/2016/8496798.
[47] V. Vinila, J. Isac, Synthesis and structural studies of superconducting perovskite GdBa2Ca3Cu4O10.5+δ nanosystems (2022) 319–341, https://doi.org/10.1016/B978-0-12-820558-7.00022-4.
[48] P. Kumar, P. Kumar, Removal of cadmium (Cd-II) from aqueous solution using gas industry-based adsorbent, SN Appl. Sci. 1 (2019), https://doi.org/10.1007/s42452-019-0377-8.
[49] A. Siregar, R. Manurung, T. Taslim, Synthesis and characterization of sodium silicate produced from corncobs as a heterogeneous catalyst in biodiesel production, Indonesian Journal of Chemistry 21 (2020) 88, https://doi.org/10.22146/ijc.53057.
[50] P. Kumar, V.S. P M, V.K. Vijay, Assessment of pyrolysis-kinetics of corncob and eucalyptus biomass residue using thermogravimetric analysis, Int. J. Sustain. Energy 40 (2021) 1–13, https://doi.org/10.1080/14786451.2021.1887186.
[51] C. Mohod, J. Dhote, Review of heavy metals in drinking water and their effect on human health, International Journal of Innovative Research in Science, Engineering and Technology 2 (7) (2013) 2992–2996. www.ijirset.com.
[52] C. Grandclement, I. Seyssiecq, A. Piram, P. Wong-Wah-Chung, G. Vanot, N. Tiliacos, N. Roche, P. Doumenq, From the conventional biological wastewater treatment to hybrid processes, the evaluation of organic micropollutant removal: a review, Water Res. 111 (2017) 297–317, https://doi.org/10.1016/j.watres.2017.01.005.
[53] B.K. Olkeba, A. Beyene, F. Fufa Feyessa, M. Megersa, M. Behm, Experimental evaluation of sorptive removal of fluoride from drinking water using iron ore, Appl. Water Sci. 6 (2014) 57–65, https://doi.org/10.1007/s13201-014-0210-x.